# Experimental deformation of olivine single crystals at lithospheric temperatures

Sylvie Demouchy, S. E. Schneider, S. J. Mackwell, M. E. Zimmerman, D. L. Kohlstedt

# Experimental deformation of olivine single crystals at lithospheric temperatures

Sylvie Demouchy,[1,2,3] Stephen E. Schneider,[2] Stephen J. Mackwell,[1]
Mark E. Zimmerman,[2] and David L. Kohlstedt[2]

Received 11 November 2008; revised 14 December 2008; accepted 17 December 2008; published 21 February 2009.

[1] Rheological properties of mantle minerals and rocks at temperatures ($T$) appropriate to much of Earth's lithosphere have remained poorly constrained, even though past experimental studies on olivine single crystals and polycrystalline aggregates have quantified the high-temperature creep mechanisms ($T >$ 1200°C). Consequently, we have performed deformation experiments on crystals of San Carlos olivine at lower temperatures, from 900° to 1200°C, in triaxial compression along the $[101]_c$ direction. The experiments were carried out at a confining pressure of 300 MPa in a high-resolution gas-medium mechanical testing apparatus at differential stresses of 100 to 500 MPa. Several samples were deformed at constant displacement rate and others at constant load, in order to provide insight into possible effects of work-hardening. Under the deformation conditions investigated, little evidence of work-hardening was observed. The data follow a power-law dependence on stress, as in previous high-temperature deformation studies. The samples were, however, considerably weaker than predicted by the experimentally determined high-temperature constitutive equation for olivine crystals of this orientation from the study of Bai et al. (1991). The mechanical behavior correlates instead with the weaker of the two mechanisms (flow laws) that contribute to the high-temperature constitutive equation. Thus, our experiments demonstrate that published high-temperature constitutive equations overestimate the strength of lithospheric mantle and that the transition to low-temperature creep occurs at lower temperatures than previously inferred. **Citation:** Demouchy, S., S. E. Schneider, S. J. Mackwell, M. E. Zimmerman, and D. L. Kohlstedt (2009), Experimental deformation of olivine single crystals at lithospheric temperatures, *Geophys. Res. Lett.*, *36*, L04304, doi:10.1029/2008GL036611.

## 1. Introduction

[2] The strength of the mantle lithosphere is largely controlled by the rheological properties of its dominant mineral, olivine, which makes up between 40 and 80% of its volume. At high temperatures, rheological behavior is well described by a constitutive equation composed of one or a combination of power-law flow laws, each of which expresses the strain rate as a function of thermomechanical and microstructural parameters, including stress, pressure, temperature, silica activity, water and oxygen fugacity, and grain size. For single crystals of olivine, a complete set of constitutive equations exists over a wide range of thermodynamic conditions based on one-atmosphere, compressional creep experiments [*Kohlstedt and Goetze*, 1974; *Durham and Goetze*, 1977; *Durham et al.*, 1985; *Bai et al.*, 1991; *Bai and Kohlstedt*, 1992]. These authors investigated flow on the dominant high-temperature slip systems by deforming San Carlos olivine crystals parallel to the $[101]_c$, $[110]_c$ and $[011]_c$ directions. Here, the notation $[101]_c$ indicates a crystal compressed along a direction 45° to the [100] and [001] axes and 90° to the [010] axis; the subscript "c" denotes directions oriented relative to a fictitious cubic lattice as distinct from the orthorhombic lattice of olivine. For polycrystalline samples of olivine, the effects of stress, temperature, and water fugacity on high-temperature flow behavior have been studied as well [*Carter and Ave'Lallemant*, 1970; *Chopra and Paterson*, 1984; *Karato et al.*, 1986; *Borch and Green*, 1989; *Mei and Kohlstedt*, 2000; *Boettcher et al.*, 2007].

[3] At the lower temperatures and higher differential stresses relevant for the lithosphere, other types of flow behavior are observed. *Phakey et al.* [1972] used a solid-medium deformation apparatus to deform single crystals of olivine at temperatures from 600° to 1250°C. These constant strain rate tests exhibited work hardening, especially at lower temperatures. The pioneering study on the low-temperature strength of olivine by *Evans and Goetze* [1979] employed micro-indentation tests from room temperature to 780°C on single crystal and polycrystalline samples to obtain the first low-temperature rheological laws for olivine. They also demonstrated a transition from low-temperature to high-temperature creep behavior over the range from around 900° to 1200°C in hot-hardness indentation experiments. Recently, *Raterron et al.* [2004] performed load relaxation experiments on polycrystalline samples of olivine at pressures from 4.9–9.2 GPa using a DIA cubic anvil press coupled with X-ray diffraction and X-ray radiograph measurements within a synchrotron to estimate in situ differential stress and strain, respectively. While this study resulted in a flow law for olivine at low temperature (500°–740°C) that yields mechanical behavior notably weaker than that of *Evans and Goetze* [1979], direct comparison is limited by the significant differences in confining pressure and the lack of a well-defined activation volume for low-temperature creep.

[4] While deformation of olivine at high temperatures ($\gtrsim$1200°C) can be described by power-law constitutive equations and deformation at low temperatures ($\lesssim$700°C) can be fit by an exponential-law constitutive equation,

[1]Lunar and Planetary Institute, Houston, Texas, USA.
[2]Department of Geology and Geophysics, University of Minnesota, Minneapolis, Minnesota, USA.
[3]Now at Géosciences Montpellier, Université Montpellier 2, CNRS, Montpellier, France.


0094-8276/09/2008GL036611

deformation at intermediate temperatures is less well defined. Although the lowest temperature data from *Bai et al.* [1991], *Durham and Goetze* [1977], and *Mackwell et al.* [1985] suggest weakening relative to the high-temperature flow laws, the data appear consistent with power-law behavior and the microstructures are similar to those observed for the higher-temperature samples. Thus, a reevaluation of the mechanical behavior of olivine at temperatures between 700° and 1200°C is necessary, especially considering the importance of this temperature range in defining flow in Earth's lithospheric mantle.

[5] The present study aims to extend previous high-temperature deformation results for single crystals of olivine by *Bai et al.* [1991] to lower temperatures and higher differential stresses by taking advantage of the high-resolution capabilities of a gas-medium deformation apparatus. Results of these experiments help constrain the strength of olivine at the lower temperatures and higher differential stresses relevant to Earth's lithospheric mantle.

## 2. Experimental Methods

### 2.1. Sample Preparation

[6] Gem-quality crystals of San Carlos olivine with a composition of $(Mg_{0.91}Fe_{0.09}Ni_{0.003})_2SiO_4$ were oriented crystallographically using Laue back reflection x-ray diffraction. Cylinders 2.2 mm in diameter and 3.2 to 5.2 mm in length were cored with long axes parallel to $[101]_c$. Fourier transform infrared analyses revealed <10 H/$10^6$Si (for analytical details, see *Demouchy et al.* [2007]). For experiments at $T \geq 1000$°C, the samples were placed into thick-walled cylindrical sleeves of nickel with an outer diameter of 10 mm and heights equal to those of the samples. For experiments at $T < 1000$°C, silver was used as the sleeve material, which supported a negligible portion of the load (~2 MPa at 800°C, see auxiliary material Table S1).[1] To determine the contribution of the sample jacket to the measured load, flow laws for iron, nickel and silver were obtained from *Frost and Ashby* [1982] and checked against two constant displacement rate experiments performed using Ni and Ag plugs (Table S1). To buffer oxygen fugacity and silica activity, each cylinder of olivine was coated with a mixture of Ni plus NiO and powdered enstatite, dried under vacuum, and placed into its nickel or silver sleeve. A 30-$\mu$m thick disc of nickel was placed at either end of the sample sleeve. This sample assembly was then encapsulated along with zirconia and alumina pistons inside an iron jacket [*Mei and Kohlstedt*, 2000].

### 2.2. Deformation Experiments

[7] Seven triaxial compressive deformation experiments at constant displacement rate or constant load were performed at $900° \leq T \leq 1200$°C on olivine crystals using a high-resolution gas-medium high-pressure apparatus with an uncertainty in differential stress of <5 MPa. The confining pressure was 300 ± 1 MPa. Run temperature varied by <2°C along the length of the sample. Temperature was increased at a rate of ~50°C/min at the start and decreased to 300°C within 15 min at the end of an experiment at which point the load was removed. This procedure minimized loss of the dislocation microstructure after cessation of deformation. Values of stress and strain rate were corrected for changes in cross-sectional area during deformation assuming that samples maintained a cylindrical shape.

## 3. Results

[8] A summary of experimental conditions and mechanical data are provided in Table S1. The mechanical response of an olivine crystal (PI-1322) deformed at constant displacement rate at $T = 1000$°C is illustrated in Figure 1. The increase in strength with increasing strain likely reflects inhomogeneous strain distribution in the samples due to frictional end effects that cause barreling in the middle of the sample. Such effects result in an overestimate of the calculated stress when the homogeneous deformation model is used to correct for sample shortening [*Moosbrugger*, 2002]. In general, there is little evidence for work-hardening in our samples. After deformation, some samples contained a few fractures that formed during unloading at the end of the experiments.

[9] All results from this study are plotted in Figure 2, including a more recent result (PI-1424) at 1200°C [*Schneider*, 2008]. The 900°C experiment, performed at a constant displacement rate, yielded a steady state differential stress of 470 MPa to a strain of ~15%; above this strain, the sample strengthened to ~530 MPa at a strain of 22%. While much of this apparent strengthening may be an artifact of the barreling of the sample at high strain, it may also reflect incipient work-hardening. Given the limited number of samples and range of experimental conditions, we cannot justify fitting a flow law to the data. Instead, we compared the data to the high-temperature constitutive equation from *Bai et al.* [1991]. The solid line in Figure 2 is the constitutive equation for $[101]_c$ crystals at 1000°C, a combination of two power-law flow laws, each corresponding to an independent deformation mechanism. According to the constitutive equation formulated by *Bai et al.* [1991], the

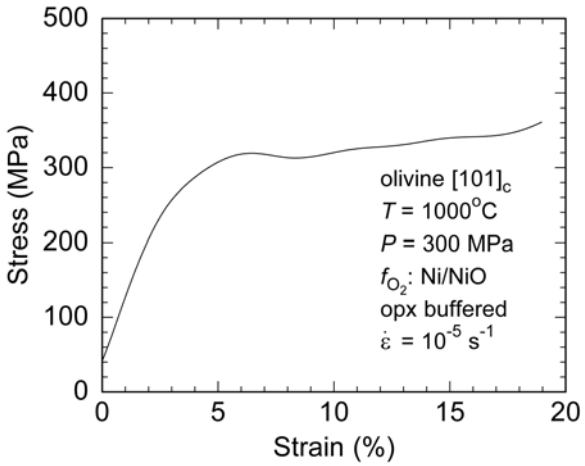


**Figure 1.** Plot of differential stress versus strain for constant displacement rate experiment PI-1322 at 1000°C. The stress has been corrected for changes in sample dimensions during deformation and to a constant strain rate of $10^{-5}$ $s^{-1}$ using a stress exponent of $n = 3.5$.

[1] Auxiliary materials are available in the HTML. doi:10.1029/2008GL036611.

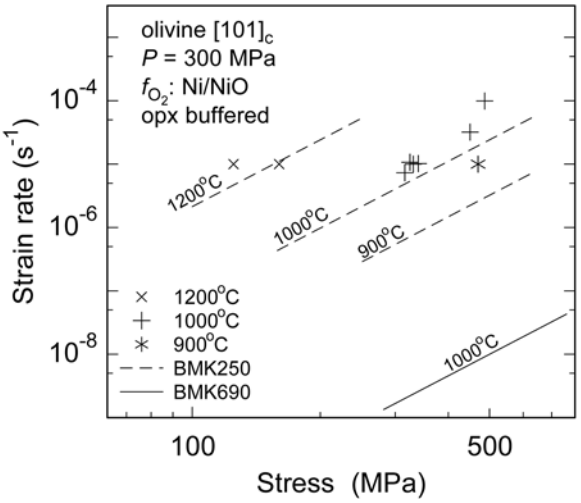


**Figure 2.** Log-log plot of strain rate versus differential stress for all of the olivine crystals deformed in this study. The solid line is the *Bai et al.* [1991] constitutive equation at 1000°C for $[101]_c$ olivine crystals. This line also corresponds to the stronger of the two flow laws that contribute to high-temperature creep of $[101]_c$ crystals (BMK690 [from *Bai et al.*, 1991]). The dashed lines correspond to the weaker of the two flow laws for temperatures of 900°, 1000° and 1200°C (BMK250 [from *Bai et al.*, 1991]). The flow laws were calculated for olivine buffered by orthopyroxene at an oxygen fugacity corresponding to the Ni/NiO buffer at the appropriate temperature. These laws were corrected from room pressure to a confining pressure of 300 MPa using an activation volume of $2.0 \times 10^{-5}$ $m^3$/mol [*Hirth and Kohlstedt*, 2003].

stronger of the two mechanisms controls the mechanical behavior. Under these conditions, the stronger of the two flow laws, with an activation energy of 690 kJ/mol, yields essentially the same curve as the constitutive equation. The dashed lines for temperatures of 900°, 1000°, and 1200°C describe the weaker of the two flow laws, with an activation energy of 250 kJ/mol. While the higher temperature data fit well to the dashed lines, the 900°C data point is weaker than predicted by the flow law.

## 4. Discussion

[10] Results from previous investigations of plastic flow in olivine have been analyzed in terms of flow laws describing steady-state deformation. At low temperatures ($T \lesssim 1200$°C for olivine), plastic flow of crystalline materials is often described in terms of dislocation glide resisted by lattice friction, that is, the Peierls stress, with an exponential-law equation [*Evans and Goetze*, 1979; *Frost and Ashby*, 1982]

$$\dot{\varepsilon} = \mathrm{A}\exp\left\{-\frac{Q_\mathrm{P}}{\mathrm{R}T}\left[1-\left(\frac{\sigma}{\sigma_\mathrm{P}}\right)^p\right]^q\right\}, \quad (1)$$

where R is the gas constant, A a material-dependent parameter, $Q_\mathrm{P}$ activation energy, and $\sigma$ differential stress. In equation (1), the Peierls stress, $\sigma_\mathrm{P}$, is defined as [*Peierls*, 1940; *Nabarro*, 1947]

$$\sigma_\mathrm{P} = \mathrm{B}\exp(-4\pi\xi/b),$$

where $\xi$ is the dislocation half-width, $b$ the Burgers vector, and for an edge dislocation $\mathrm{B} = 2\mu/(1-\nu)$, with $\mu$ shear modulus and $\nu$ Poisson's ratio. Values of $p$ and $q$ are empirically determined and are generally bracketed by $0 \le p \le 1$ and $1 \le q \le 2$ [*Frost and Ashby*, 1982].

[11] At high temperatures ($T \gtrsim 1200$°C for olivine), steady-state deformation is usually described by a the power-law equation [*Frost and Ashby*, 1982]

$$\dot{\varepsilon} = \mathrm{C}\sigma^n \exp(-Q_c/\mathrm{R}T). \quad (2)$$

In equation (2), $Q_c$ is the activation energy for creep, $n$ the stress exponent, and C a material-dependent parameter. For olivine single crystals, high-temperature behavior has been modeled well by constitutive equations formed by the combination of two or three power-law equations, each of the form of equation (2) [*Bai et al.*, 1991]. The *Bai et al.* [1991] constitutive equations are consistent with the behavior of dunite, which lies intermediate between the weaker and stronger of the active slip systems [*Hirth and Kohlstedt*, 2003]. Low-temperature aggregate behavior has generally been modeled using the flow law (equation (1)) from *Evans and Goetze* [1979]. In Figure 3, our single crystal data are weaker than the extrapolation of the *Bai et al.* [1991] constitutive equation for the $[101]_c$ orientation

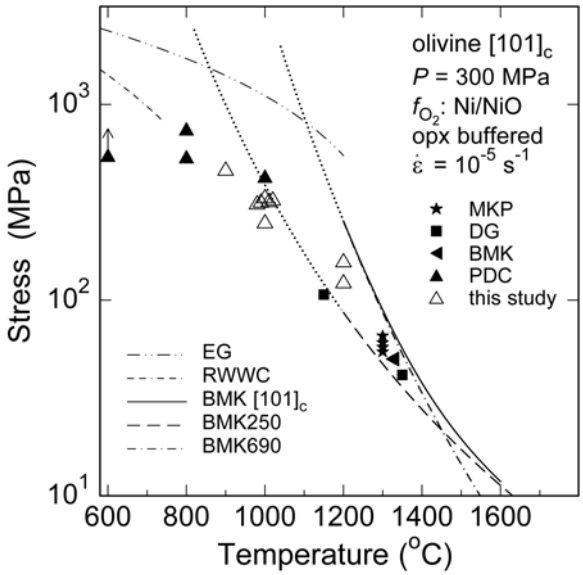


**Figure 3.** Semi-log plot of differential stress versus temperature for samples deformed in this study corrected to a strain rate of $10^{-5}$ $s^{-1}$ using a stress exponent of $n = 3.5$. Included in this plot are data from previous studies on $[101]_c$ oriented olivine single crystals from MKP, *Mackwell et al.* [1985]; DG, *Durham and Goetze* [1977]; BMK, *Bai et al.* [1991]; and PDC, *Phakey et al.* [1972]. Also plotted are the low-temperature constitutive equations for polycrystalline samples from EG [*Evans and Goetze*, 1979] and RWWC [*Raterron et al.*, 2004]. In addition, the *Bai et al.* [1991] constitutive equation for olivine crystals deformed along the $[101]_c$ direction (BMK), as well as the flow laws BMK690 and BMK250, are shown; these flow laws were corrected to a pressure of 300 MPa using an activation volume of $2.0 \times 10^{-5}$ $m^3$/mol. The dotted lines illustrate the extrapolation of the flow laws beyond their range of measurement.

and are weaker than the extrapolation of the *Evans and Goetze* [1979] low-temperature exponential law. They are, however, consistent with the previous experimental single-crystal data obtained at lower temperatures by *Phakey et al.* [1972], *Durham and Goetze* [1977], *Mackwell et al.* [1985], and *Bai et al.* [1991]. Also, our data and previous data at 1000° to 1200°C fit very well to the weaker of the two *Bai et al.* [1991] flow laws (BMK250 in Figures 2 and 3) that contribute to the high-temperature $[101]_c$ constitutive equation. Below 1000°C, the data fall below this curve and converge toward the low-temperature polycrystalline results from *Evans and Goetze* [1979] and *Raterron et al.* [2004].

[12] As noted above, the *Bai et al.* [1991] constitutive equation for the $[101]_c$ orientation is composed of two flow laws, the stronger of which (BMK690 in Figures 2 and 3) dominates the mechanical behavior at $T < 1450$°C [*Bai et al.*, 1991; *Bai and Kohlstedt*, 1992]. Therefore, the rate of deformation is controlled by whichever mechanism is stronger. Here, we observe that at lower temperatures the stronger mechanism is no longer required for deformation of the single crystals and that the weaker mechanism (BMK250 in Figures 2 and 3) provides a good fit to the data. Such a loss of requirement for the stronger of the two mechanisms may reflect activity of a third process at lower temperatures that is not providing significant strain at higher temperature. This process most likely has an activation energy that is lower than the 250 kJ/mol measured for the easier deformation mechanism (BMK250 in Figures 2 and 3).

[13] Dislocation microstructures provide significant insight into the microscale processes that control deformation and fix the parameters in the flow laws. At high temperatures and high oxygen fugacities, *Bai and Kohlstedt* [1992] identified the motion of dislocations with [100] Burgers vectors as predominant for deformation parallel to $[101]_c$, with near-edge dislocations zigzagging along $\langle 110 \rangle$ directions and few screw dislocations. At more reducing conditions, the majority of dislocations are long, very straight [100] screw dislocations and curved edge [100] dislocations gliding on (001); some [001] screw dislocations gliding on (100) were also identified. While it is much harder to characterize the active slip systems in low-temperature experiments, the most profound difference between high- and low-temperature deformation is the predominance of [100] dislocations at temperatures above 1200°C [*Bai and Kohlstedt*, 1992] and [001] dislocations (both edge and screw) at temperatures below 1000°C [*Goetze*, 1978; *Phakey et al.*, 1972]. In their modeling study for $[101]_c$ samples, *Durinck et al.* [2007] reported a transition from predominance of [100] dislocations at 1127°C to predominance of [001] dislocations at 927°C. The transitional region between 1000° and 1100°C is characterized by dislocations with both [100] and [001] Burgers vectors. This activation of [001] dislocations may well obviate the need for the stronger of the two high-temperature deformation mechanisms (BMK690) at temperatures below ~1200°C.

## 5. Implications

[14] The results of these experiments demonstrate that the transition from high-temperature power-law creep in olivine (equation (2)) to low-temperature exponential-law deformation (equation (1)) cannot be modeled simply as a summation of contributions from high- and low-temperature constitutive equations. This added complexity is evident from the deviation of our experimental data from the extrapolation of the *Bai et al.* [1991] constitutive equation in Figure 3 and is likely due to an evolution of the dominant dislocation Burgers vector from [100] at temperatures >1200°C to [001] at temperatures ≲900°C. This transition occurs at significantly lower temperatures than inferred from previous studies [e.g., *Evans and Goetze*, 1979] but is consistent with the results of the dislocation modeling study of *Durinck et al.* [2007].

[15] In modeling flow in the mantles of Earth and other terrestrial planets, it is usual to use experimental flow laws for olivine-rich rocks [*Kohlstedt et al.*, 1995; *Kohlstedt and Mackwell*, 2008]. The variation of rock strength as a function of depth is often illustrated by a strength envelope diagram, where higher rock strength at shallower depths corresponds to the lithosphere, which is underlain by a weaker asthenosphere. The mechanical behavior in the latter region is dominated by high-temperature creep behavior, while deformation of the lithosphere involves both high- and low-temperature creep processes. The results of the present study provide new insight into the strength of and mechanical processes in the part of the lower lithosphere where only plastic deformation processes are active. Our results cannot be applied quantitatively, as we only measured the slip systems activated in $[101]_c$-oriented olivine, and aggregate flow is a complex summation of dislocation glide and climb on all of the active slip systems. As dislocations with [001] Burgers vectors become dominant at lower temperatures, some high-temperature slip systems, including those we have not measured, will contribute less to aggregate behavior while others increase in importance. Nonetheless, at lithospheric temperatures of 900° to 1200°C, our results clearly show that olivine is weaker than previously inferred.

[16] **Acknowledgments.** S.D. is grateful to Patrick Cordier for useful discussions. S.D. and S.J.M. were supported under NASA CAN NNX08AC28A; S.E.S., M.E.Z., and D.L.K. were supported by NASA grant NNX07AP68G. LPI publication 1453.

## References

Bai, Q., and D. L. Kohlstedt (1992), High-temperature creep of olivine single crystals, 2. dislocation structures, *Tectonophysics*, *206*, 1–29.

Bai, Q., S. J. Mackwell, and D. L. Kohlstedt (1991), High-temperature creep of olivine single crystals: 1. Mechanical results for buffered samples, *J. Geophys. Res.*, *96*, 2441–2463.

Boettcher, M., G. Hirth, and B. Evans (2007), Olivine friction at the base of oceanic seismogenic zones, *J. Geophys. Res.*, *112*, B01205, doi:10.1029/2006JB004301.

Borch, R. S., and H. W. Green II (1989), Deformation of peridotite at high pressure in a new salt cell: comparison of traditional and homologous temperature treatments, *Phys. Earth Planet. Inter.*, *55*, 269–276.

Carter, N. L., and H. G. Ave'Lallemant (1970), High-temperature flow of dunite and peridotite, *Geol. Soc. Am. Bull.*, *81*, 2181–2202.

Chopra, P. N., and M. S. Paterson (1984), The role of water in the deformation of dunite, *J. Geophys. Res.*, *89*, 7861–7876.

Demouchy, S., S. J. Mackwell, and D. L. Kohlstedt (2007), Influence of hydrogen on Fe–Mg interdiffusion in (Mg,Fe)O and implications for Earth's lower mantle, *Contrib. Mineral. Petrol.*, *154*, 279–289.

Durham, W. B., and C. Goetze (1977), Plastic flow of oriented single crystals of olivine: 1. Mechanical data, *J. Geophys. Res.*, *82*, 5737–5753.

Durham, W. B., D. L. Ricoult, and D. L. Kohlstedt (1985), Interaction of slip systems in olivine, in *Point Defects in Minerals*, *Geophys. Monogr. Ser.*, vol. 31, edited by R. N. Schock, pp. 185–193, AGU, Washington, D. C.

Durinck, J., B. Devincre, L. Kubin, and P. Cordier (2007), Modeling the plastic deformation of olivine by dislocation dynamics simulations, *Am. Mineral.*, *92*, 1346–1357.

Evans, B., and C. Goetze (1979), The temperature variation of hardness of olivine and its implication for polycrystalline yield stress, *J. Geophys. Res.*, *84*, 5505–5524.

Frost, H. J., and M. F. Ashby (1982), *Deformation Mechanism Maps: The Plasticity and Creep of Metals and Ceramics*, 166 pp., Pergamon, Oxford, U. K.

Goetze, C. (1978), The mechanisms of creep in olivine, *Philos. Trans. R. Soc. London, Ser. A*, *288*, 99–119.

Hirth, G., and D. L. Kohlstedt (2003), Rheology of the upper mantle and the mantle wedge: A view from the experimentalists, in *Inside the Subduction Factory*, *Geophys. Monogr. Ser.*, vol. 138, edited by J. Eiler, pp. 83–105, AGU, Washington, D. C.

Karato, S. I., M. S. Paterson, and J. D. Fitz Gerald (1986), Rheology of synthetic olivine aggregates: Influence of grain size and water, *J. Geophys. Res.*, *91*, 8151–8176.

Kohlstedt, D. L., and C. Goetze (1974), Low-stress high-temperature creep in olivine single crystals, *J. Geophys. Res.*, *79*, 2045–2051.

Kohlstedt, D. L., and S. J. Mackwell (2008), Strength and deformation of planetary lithospheres, in *Planetary Tectonics*, edited by R. Schultz and T. Watters, Cambridge University Press, Cambridge, U.K., in press.

Kohlstedt, D. L., B. Evans, and S. J. Mackwell (1995), Strength of the lithosphere: Constraints imposed by laboratory experiments, *J. Geophys. Res.*, *100*, 17,587–17,602.

Mackwell, S. J., D. L. Kohlstedt, and M. S. Paterson (1985), The role of water in the deformation of olivine single crystals, *J. Geophys. Res.*, *90*, 11,319–11,333.

Mei, S., and D. L. Kohlstedt (2000), Influence of water on the plastic deformation of olivine aggregates: 2. Dislocation creep regime, *J. Geophys. Res.*, *105*, 21,471–21,481.

Moosbrugger, C. (2002), Representation of stress-strain behavior, in *Atlas of Stress-Strain Curves*, edited by Y. Tamarin, 2nd ed., pp. 9–10, ASM Int., Materials Park, Ohio.

Nabarro, F. R. N. (1947), Dislocations in a simple cubic lattice, *Proc. Phys. Soc.*, *59*, 256–272.

Peierls, R. E. (1940), The size of a dislocation, *Proc. Phys. Soc.*, *52*, 34–37.

Phakey, P., G. Dollinger, and J. Christie (1972), Transmission electron microscopy of experimentally deformed olivine crystals, in *Flow and Fracture of Rocks: The Griggs Volume*, *Geophys. Monogr. Ser.*, vol. 16, edited by H. C. Heard et al., pp. 117–138, AGU, Washington, D. C.

Raterron, P., Y. Wu, D. J. Weidner, and J. Chen (2004), Low-temperature olivine rheology at high pressure, *Phys. Earth Planet. Inter.*, *145*, 149–159.

Schneider, S. E. (2008), Low-temperature deformation of olivine single crystals, M.S. thesis, 104 pp., Univ. of Minn., Minneapolis.

S. Demouchy, Géosciences Montpellier, UMR 5243, UMII, cc.60, Université Montpellier 2, CNRS, F-34095 Montpellier CEDEX, France.

D. L. Kohlstedt, S. E. Schneider, and M. E. Zimmerman, Department of Geology and Geophysics, University of Minnesota, 310 Pillsbury Drive SE, Minneapolis, MN 55455, USA. (dlkohl@tc.umn.edu)

S. J. Mackwell, Lunar and Planetary Institute, 3600 Bay Area Boulevard, Houston, TX 77058, USA.